

# Stability of the Atlantic Meridional Overturning Circulation: A Model Intercomparison

Andrew J. Weaver<sup>a</sup>, Jan Sedláček<sup>b</sup>, Michael Eby<sup>a</sup>,  
Kaitlin Alexander<sup>a</sup>, Elisabeth Cressin<sup>c</sup>, Thierry Fichefet<sup>c</sup>, Gwenaëlle Philippon-Berthier<sup>c</sup>,  
Fortunat Joos<sup>d,e</sup>, Michio Kawamiya<sup>f</sup>, Katsumi Matsumoto<sup>g</sup>, Marco Steinacher<sup>d,e</sup>, Kaoru Tachiiri<sup>f</sup>,  
Kathy Tokos<sup>g</sup>, Masakazu Yoshimori<sup>h</sup>, Kirsten Zickfeld<sup>i</sup>

<sup>a</sup> School of Earth and Ocean Sciences, University of Victoria, Victoria, British Columbia, Canada

<sup>b</sup> Institute for Atmospheric and Climate Science, ETH, Zurich, Switzerland

<sup>c</sup> Earth and Life Institute, Georges Lemaître Centre for Earth and Climate Research, Université  
Catholique de Louvain, Louvain-La-Neuve, Belgium

<sup>d</sup> Climate and Environmental Physics, Physics Institute, University of Bern, Bern, Switzerland

<sup>e</sup> Oeschger Centre for Climate Change Research, University of Bern, Bern, Switzerland

<sup>f</sup> Research Institute for Global Change, JAMSTEC, Yokohama, Japan

<sup>g</sup> University of Minnesota, Minneapolis

<sup>h</sup> Atmosphere and Ocean Research Institute, University of Tokyo.

<sup>i</sup> Simon Fraser University, Vancouver, British Columbia, Canada

Submitted to:

**Geophysical Research Letters**

July, 2012

## 31   **Abstract**

32   The evolution of the Atlantic Meridional Overturning Circulation (MOC) in 30 models of varying  
33   complexity is examined under four distinct Representative Concentration Pathways. The models  
34   include 25 Atmosphere-Ocean General Circulation Models (AOGCMs) or Earth System Models  
35   (ESMs) that submitted simulations in support of the 5<sup>th</sup> phase of the Coupled Model Intercomparison  
36   Project (CMIP5) and 5 Earth System Models of Intermediate Complexity (EMICs). All models  
37   projected very similar behavior during the 21<sup>st</sup> century. Over this period the strength of MOC reduced  
38   by a best estimate of 22% (18% - 25%; 5%-95% confidence limits) for RCP2.6, 26% (23% - 30%) for  
39   RCP4.5, 29% (23% - 35%) for RCP6.0 and 40% (36 % - 44%) for RCP8.5. While two of the models  
40   eventually realized a slow shutdown of the MOC under RCP8.5, no model exhibited an abrupt change  
41   of the MOC. Through analysis of the freshwater flux across 30°-32°S into the Atlantic, it was found  
42   that more than half of the CMIP5 models were in a bistable regime of the MOC for the duration of their  
43   RCP integrations. The results support previous assessments that it is very unlikely that the MOC will  
44   undergo an abrupt change to an off state as a consequence of global warming.

45

## 46   **1. Introduction**

47   In the 4<sup>th</sup> Assessment Report of the Intergovernmental Panel on Climate Change (IPCC AR4) the  
48   Atlantic Meridional Overturning Circulation (MOC) was described as being *very unlikely* to undergo  
49   an abrupt (over the period of a decade or two) shutdown in the 21<sup>st</sup> century [Meehl *et al.*, 2007b]. This  
50   assessment was based on a basic understanding of processes involved in past abrupt changes of the  
51   MOC [e.g., Clarke *et al.*, 2002; Alley *et al.*, 2003], focused model intercomparison projects [e.g.,  
52   Gregory *et al.*, 2005; Rahmstorf *et al.*, 2005; Stouffer *et al.*, 2006] as well as coupled model simulations  
53   conducted as part of the third phase of the Coupled Model Intercomparison Project [CMIP3; Meehl *et al.*  
54   *et al.*, 2007a]. The IPCC AR4 further argued that it was too early to make an assessment regarding the  
55   stability of the MOC beyond the 21<sup>st</sup> century.

56

57   Concomitant with and subsequent to the release of the AR4, the US Climate Change Science Program  
58   (CCSP) initiated the preparation of 21 synthesis and assessment products designed to provide decision  
59   makers in the United States the latest information on a variety of climate-related scientific issues of  
60   strategic national importance. One of these, Synthesis and Assessment Product (SAP) 3.4 (CCSP,  
61   2008), focused on the issue of Abrupt Climate Change. In SAP 3.4, Delworth *et al.* [2008] reaffirmed  
62   the assessment of Meehl *et al.* [2007b] that it is very unlikely that the Atlantic MOC will abruptly

63 change in the 21<sup>st</sup> century, even though the MOC was expected to weaken by a best estimate of 25%-  
64 30%. However, they further concluded that it was also unlikely that global warming would lead to a  
65 MOC collapse beyond the end of the 21st century, although they were not able to completely exclude  
66 this possibility.

67

68 As originally discussed in the pioneering work of *Stommel* [1961], *Rooth* [1982] and *Bryan* [1986], salt  
69 transported poleward in the North Atlantic provides a potentially destabilizing advective feedback to  
70 the MOC. That is, if the strength of the MOC were to reduce, then less salt would be transported into  
71 the North Atlantic thereby encouraging further reduction in its strength. The existence of this slow, salt  
72 advection feedback is critical to the presence of stable multiple equilibria of the MOC [see *Rahmstorf*,  
73 1996]. Further analysis has determined that the sign of net freshwater flux transported by the MOC into  
74 the Atlantic across 30°-32°S serves as a key measure of this salt advection feedback and hence an  
75 indicator of the potential existence of multiple equilibria [*Rahmstorf*, 1996; *Gregory et al.*, 2003; *De*  
76 *Vries and Weber*, 2005; *Dijkstra*, 2007; *Weber et al.*, 2007; *Huisman et al.*, 2010; *Drijfhout et al.*,  
77 2011; *Hawkins et al.*, 2011]. A negative freshwater flux associated with the zonally-integrated  
78 baroclinic flow across 30°-32°S indicates net salt import to the Atlantic by the MOC. This in turn  
79 reveals the presence of the potentially destabilizing salt advection feedback and hence the existence of  
80 multiple equilibria. That is, the system is in a bistable regime. Conversely, if the freshwater flux is  
81 positive, the system is in a monostable regime.

82

83 Since the publication of both the IPCC and CCSP assessments a number of studies have argued that  
84 many of the CMIP3 models might be overly stable [e.g., *Hofmann and Rahmstorf*, 2009; *Drijfhout et*  
85 *al.*, 2011). This is significant since if the models are predominantly in a monostable regime for the  
86 present climate, then they will invariably project a MOC that would reestablish itself after a small  
87 perturbation caused it to weaken. At the same time, observations suggest that the present-day Atlantic  
88 is in a bistable regime [*Weijer et al.*, 1999; *Huisman et al.*, 2010; *Hawkins et al.*, 2011]. As the  
89 potential climatic and societal impact of an abrupt change of the MOC would be profound [*Kuhlbrodt*  
90 *et al.*, 2009], determining the stability properties of the MOC in models is a matter of some importance.  
91 In light of the availability of a new collection of model results from the fifth phase of the Coupled  
92 Model Intercomparison Project [CMIP5; *Taylor et al.*, 2012] as well as from an intercomparison  
93 project involving Earth System Models of Intermediate Complexity (EMICs) conducted in support of

the IPCC 5<sup>th</sup> Assessment Report [*Eby et al.*, 2012], it is evidently timely to reexamine the stability of the MOC within this new generation of models.

## 2. Description of the model experiments

The results from 30 Atmosphere-Ocean General Circulation Models (AOGCMs), Earth System Models (ESMs) and EMICs were analysed for this study. All models followed the CMIP5 protocol [*Taylor et al.*, 2012] for their historical integrations from 1850 to 2005. During this period, changes in both natural and anthropogenic forcing (including land surface changes) were prescribed. From 2006 to 2300, the models were forced with specified trace gas and aerosol concentrations or emissions following, and consistent with, the Representative Concentration Pathways (RCPs) detailed in *Moss et al.* [2010]. These RCPs are distinguished by either their eventual stabilization level of anthropogenic radiative forcing (RCP4.5 and RCP 6.0) or, in the case of RCP2.6 and RCP8.5, their radiative forcing at 2100 (Figure 1a).

All of the models completed the RCP4.5 integration to year 2100. Only 26 of them completed RCP8.5, 21 undertook RCP2.6 and 18 RCP6.0. Several of the models completed the RCP extensions to year 2300 (see Table 1). While velocity and tracer output were available from many of the CMIP5 model simulations, the maximum strength of the Atlantic MOC was updated to the CMIP5 database by fewer of them. In the analysis that follows, for each model, a single timeseries of the Atlantic MOC was obtained by averaging over all members of any submitted model ensemble. For the EMICs this was also done in the calculation of the baroclinic freshwater transport by the MOC into the Atlantic ( $F_{ov}$ ) across 30°-32°S. Only the first complete ensemble member was used in the calculation of  $F_{ov}$  for the CMIP5 models.

The five participating EMICs are as follows (details and descriptions can be found in *Eby et al.*, [2012]): Bern3D (B3) from the University of Bern; LOVECLIM v1.2 (LO) from the Université Catholique de Louvain; MESMO v1.0 (ME) from the University of Minnesota; MIROC-lite-LCM (ML) from the Japan Agency for Marine-Earth Science and Technology; UVic v2.9 (UV) from the University of Victoria. Each of these EMICs extended the RCP integrations to 3000 with radiative forcing held constant from 2300-3000 at the 2300 values (see also *Zickfeld et al.*, [2012]).

## 3. Results

126 The behavior of the MOC in all models is remarkably similar over the 21<sup>st</sup> century (both CMIP5 and  
 127 EMIC) under all radiative forcing scenarios (Figure 2). All models project a weakening of the MOC  
 128 during the 21<sup>st</sup> century with a multi-model average of 22% (18% - 25%; 5%-95% confidence limits) for  
 129 RCP2.6, 26% (23% - 30%) for RCP4.5, 29% (23% - 35%) for RCP6.0 and 40% (36 % - 44%) for  
 130 RCP8.5. None of the models reveal a shutdown of the conveyor during the 21<sup>st</sup> century. As also noted  
 131 in previous analyses with both simple models [*Stocker and Schmittner, 1997*] and more complicated  
 132 ESMs [*Meehl et al., 2012*], the response of the MOC, and any potential slow spin down, depends on  
 133 both the rate and magnitude of the radiative forcing.

134  
 135 During the RCP extension period from 2100-2300, the strength of the MOC either stabilizes or starts to  
 136 recover in all the models that completed the RCP2.6, RCP4.5 and RCP6.0 simulations over this period.  
 137 Only under the RCP8.5 scenario does the MOC spin down in any model. This eventually occurs before  
 138 2200 in CNRM and after 2700 in Bern3D (Figure 2). However, both of these models also start with the  
 139 weakest Atlantic MOC during the preindustrial time.

140  
 141 As noted in the introduction, the freshwater flux by the MOC into the Atlantic through 30°-32°S ( $F_{ov}$ )  
 142 provides an important indicator as to whether the MOC is in a monstable or bistable region. This  
 143 freshwater flux across any particular latitude is given by:

$$144 \quad F_{ov} = -\frac{1}{S_0} \int_{-H}^0 \overline{v^*}(z) \langle S(z) \rangle dz, \quad (1)$$

145 where  $v$  is the northward velocity, the overbar denotes its zonal integral, the asterisk denotes its  
 146 departure from the vertical average (i.e. the baroclinic component) and the  $\langle \rangle$  denotes a zonal mean.  
 147 That is,  $\overline{v^*}(z)$  is the zonally-integrated, northward baroclinic velocity and  $\langle S(z) \rangle$  is the zonally-  
 148 averaged salinity. Here  $S_0$  is a reference salinity (selected to be 35 psu) and  $H$  is the depth of the ocean.

149  
 150 The freshwater flux  $F_{ov}$  across 30°-32°S for each of the models under each RCP is shown in Figure 3.  
 151 All but four of the models (Bern3D, GFDL-ESM2M, MESMO, MPI-ESM-LR) reveal that  $F_{ov}$  is of the  
 152 same sign throughout the entire length of the integrations across all RCPs. Thirteen of the models  
 153 always have  $F_{ov} < 0$  (bistable regime) and thirteen of the models always have  $F_{ov} > 0$  (monostable  
 154 regime) at all time and for all RCPs.

155

156 In GFDL\_ESM2M,  $F_{ov}$  oscillates about  $F_{ov} = 0$  during the historical period due to natural variability  
 157 inherent to the system (Figure 4a). However, during the later part of the 20<sup>th</sup> century,  $F_{ov}$  shifts to  
 158 become  $F_{ov} < 0$  (bistable regime) for all RCP scenarios out to 2100. In the case of MPI-ESM-LR,  
 159 RCP2.6 and RCP4.5 always remain in the bistable regime (with  $F_{ov} < 0$ ). RCP8.5, on the other hand,  
 160 trends into positive (monostable) territory from 2100 to 2300 (Figure 4b). Two of the EMICs also have  
 161  $F_{ov}$  change sign during the course of their integrations. In MESMO (Figure 4c), RCP8.5 eventually  
 162 moves from  $F_{ov} > 0$  (monostable regime) to  $F_{ov} < 0$  (bistable regime), while all other RCP integrations  
 163 remain in the monostable regime. In Bern3D, all of the RCP integrations begin with  $F_{ov} > 0$ , but in the  
 164 case of RCP4.5, RCP6.0 and RCP8.5, they eventually cross over into the bistable regime. RCP2.6  
 165 remains in the monostable regime but  $F_{ov}$  slowly drifts towards zero as the integration proceeds to year  
 166 3000. RCP8.5 reveals interesting behavior in this model, one of only two that eventually has a MOC  
 167 spin down. By about 2600,  $F_{ov}$  becomes positive again and continues to grow in an unbounded fashion  
 168 by year 3000. This suggests that in Bern 3D, the collapsed state is monostable towards the end of the  
 169 integration.

170

#### 171 4. Discussion and Conclusions

172 In our experiments we have not imposed a freshwater forcing to examine the hysteresis behaviour of  
 173 the MOC under constant radiative forcing [e.g., as in *Stocker and Wright*, 1991; *Rahmstorf et al.*, 2005].  
 174 Rather, we have explored the behaviour of the MOC under changing, and ultimately sustained radiative  
 175 forcing [e.g., *Manabe and Stouffer*, 1988; *Plattner et al.*, 2008]. The rationale for doing this was not to  
 176 use  $F_{ov}$  as a predictor of the transient, radiatively forced behavior of the MOC, but instead to determine  
 177 whether or not the salt-advection feedback would be present to allow for multiple equilibria under any  
 178 given radiative forcing. That is, we wished to determine whether or not models were in general overly  
 179 stable and preferentially lay in the monostable regime, unlike observations.

180

181 We analysed the behavior of the MOC in 30 models of varying complexity under four different  
 182 Representative Concentration Pathways. The model responses were remarkably similar over the 21<sup>st</sup>  
 183 century. All models showed a weakening of the Atlantic MOC but none showed an abrupt change to an  
 184 off state. Beyond 2100, only two models eventually exhibited an eventual spin down of the MOC but  
 185 even this shutdown occurred gradually, and not in an abrupt fashion. Previous criticism regarding a  
 186 tendency for models to be overly stable appears not to be the case in the CMIP5 and EMIC models  
 187 examined here. More than half of the CMIP5 models analysed were in a bistable regime of the MOC

during the RCP integrations. Taken together, this analysis tends to strengthen previous assessments that it is very unlikely that the MOC will undergo an abrupt transition during the 21<sup>st</sup> century. In fact, no model exhibited an abrupt transition even beyond the 21<sup>st</sup> century.

Abrupt change of the MOC was certainly a pervasive feature of the last glacial cycle (Clark et al., 2002; Alley et al., 2003). However, unlike today, vast reservoirs of freshwater were present in the Laurentide and Fennoscandian Ice Sheets and associated proglacial lakes. Sudden releases of this freshwater via either ice sheet surging, ice berg calving or meltwater discharge would affect the surface densities of the North Atlantic and could initiate a fast convective feedback that might ultimately lead to a MOC collapse. While none of the models examined in this study included an interactive Greenland Ice Sheet, *Jungclauss et al.* [2006], *Mikolajewicz et al.* [2007], *Driesschaert et al.* [2007], and *Hu et al.* [2009] all found only a slight temporary effect of increased melt water fluxes on the AMOC. This was either small compared to the effect of enhanced poleward atmospheric moisture transport in a warmer mean climate or only noticeable in the most extreme scenarios. It appears that significant ablation of the Greenland ice sheet greatly exceeding even the most aggressive of current projections would be required [*Swingedouw et al.*, 2007; *Hu et al.*, 2009] to initiate an abrupt collapse of the MOC as a consequence of global warming.

## Acknowledgements

AJW, ME and KA are grateful for ongoing support from NSERC through its Discovery Grant, G8 and CREATE programs. TF and EC acknowledge support from the Belgian Federal Science Policy Office.

## References

- Alley, R.B., et al. (2003), Abrupt climate change, *Science*, **299**, 2005-2010, doi:10.1126/science.1081056.
- Bryan, F.O. (1986), High latitude salinity effects and interhemispheric thermohaline circulations, *Nature*, **323**, 301-304.
- CCSP (2008), *Abrupt Climate Change*. A report by the U.S. Climate Change Science Program and the Subcommittee on Global Change Research, U.S. Geological Survey, Reston, VA
- Clark, P.U., N.G. Pisias, T.F. Stocker, and A.J. Weaver (2002), The role of the thermohaline circulation in abrupt climate change, *Nature*, **415**, 863-869.

219 Delworth, T.L., et al. (2008), The potential for abrupt change in the Atlantic Meridional Overturning  
220 Circulation, in *Abrupt Climate Change*. A report by the U.S. Climate Change Science Program  
221 and the Subcommittee on Global Change Research, pp. 258-359, U.S. Geological Survey,  
222 Reston, VA.

223 Dijkstra, H.A. (2007), Characterization of the multiple equilibria regime in a global ocean model,  
224 *Tellus*, **59A**, 695–705.

225 Driesschaert, E., et al. (2007), Modeling the influence of Greenland ice sheet melting on the meridional  
226 overturning circulation during the next millennia, *Geophys. Res. Lett.*, **34**, L10707,  
227 doi:10.1029/2007GL029516.

228 Drijfhout, S.S., S.L. Weber, and E. van der Waluw (2011), The stability of the MOC as diagnosed  
229 from model projections for pre-industrial, present and future climates, *Climate Dynamics*, **37**,  
230 1575-1586.

231 Eby, M., et al. (2012), Historical and idealized climate model experiments: An EMIC Intercomparison,  
232 *Climate of the Past*, submitted.

233 Gregory, J.M., O.A. Saenko, and A.J. Weaver (2003), The role of the Atlantic freshwater balance in the  
234 hysteresis of the meridional overturning circulation. *Climate Dynamics*, **21**, 707-717

235 Gregory, J.M. et al. (2005), A model intercomparison of changes in the Atlantic thermohaline  
236 circulation in response to increasing atmospheric CO<sub>2</sub> concentration, *Geophys. Res. Lett.*,  
237 **32(12)**, L12703, doi:10.1029/2005GL023209.

238 Hawkins E., R.S. Smith, L.C. Allison, J.M. Gregory, T.J. Woollings, H. Pohlmann, and B. de Cuevas  
239 (2011), Bistability of the Atlantic overturning circulation in a global climate model and links  
240 to ocean freshwater transport, *Geophys. Res. Lett.*, **38**, L10605, doi:10.1029/2011GL047208.

241 Hofmann, M., and S. Rahmstorf (2009), On the stability of the Atlantic meridional overturning  
242 circulation, *Proc. Nat. Acad. Sci.*, **106**, 20584-20589.

243 Hu, A., G.A. Meehl, W. Han, and J. Yin (2009), Transient response of the MOC and climate to  
244 potential melting of the Greenland ice sheet in the 21<sup>st</sup> century, *Geophys. Res. Lett.*, **36**,  
245 L10707, doi:10.1029/2009GL037998.

246 Huisman, S.E., M. den Toom, H.A. Dijkstra, and S. Drijfhout (2010), An indicator of the multiple  
247 equilibria regime of the Atlantic meridional overturning circulation, *J. Phys. Oceanogr.*, **40**,  
248 551-567.

249 Jungclauss, J.H., H. Haak, M. Esch, E. Roeckner, and J. Marotzke (2006), Will Greenland melting halt  
250 the thermohaline circulation? *Geophys. Res. Lett.*, **33**, L17708, doi:10.1029/2006GL026815.



251 Kuhlbrodt, T., et al. (2009), An integrated assessment of changes in the thermohaline circulation,  
 252 *Climatic Change*, **96**, 489-537.

253 Manabe, S., and R.J. Stouffer (1988), Two stable equilibria of a coupled ocean-atmosphere model, *J.*  
 254 *Climate*, **1**, 841–866.

255 Meehl, G., C. Covey, T. Delworth, M. Latif, B. McAvaney, J. Mitchell, R. Stouffer, and K. Taylor  
 256 (2007), The WCRP CMIP3 multimodel dataset, *Bull. Amer. Meteor. Soc.*, **88**, 1383–1394.

257 Meehl, G.A., et al. (2007b) Global Climate Projections, in *Climate Change 2007: The Physical Science*  
 258 *Basis. Contribution of Working Group I to the Fourth Assessment Report of the IPCC*, edited  
 259 by S. Solomon et al., pp. 747-845, Cambridge University Press, New York, NY, USA.

260 Meehl, G.A., et al. (2012), Climate system response to external forcings and climate change  
 261 projections in CCSM4, *J. Climate*, **25**, 3661-3683.

262 Mikolajewicz, U., M. Vizcaíno, J. Jungclaus, and G. Schurgers (2007), Effect of ice sheet interactions  
 263 in anthropogenic climate change simulations, *Geophys. Res. Lett.*, **34**, L18706,  
 264 doi:10.1029/2007GL031173.

265 Moss, R.H., et al. (2010), The next generation of scenarios for climate change research and assessment,  
 266 *Nature*, **463**, 747-756.

267 Plattner, G.-K., et al. (2008), Long-term climate commitments projected with climate - carbon cycle  
 268 models, *J. Climate*, **21**, 2721-2751.

269 Rahmstorf, S. (1996), On the freshwater forcing and transport of the Atlantic thermohaline circulation,  
 270 *Climate Dynamics*, **12**, 799-811.

271 Rahmstorf, et al. (2005), Thermohaline circulation hysteresis: a model intercomparison, *Geophys. Res.*  
 272 *Lett.*, **32(23)**, L23605, doi:10.1029/2005GL023655.

273 Rooth, C. (1982), Hydrology and ocean circulation, *Prog. Oceanogr.*, **11**, 131–149.

274 Stocker, T.F., and D.G. Wright (1991), Rapid transitions of the ocean’s deep circulation induced by  
 275 changes in surface water fluxes, *Nature*, **351**, 729-732.

276 Stocker, T.F., and A. Schmittner (1997), Influence of CO2 emission rates on the stability of the  
 277 thermohaline circulation, *Nature*, **388**, 862-865.

278 Stommel, H. (1961), Thermohaline convection with two stable regimes of flow. *Tellus*, **13**, 224–230.

279 Stouffer, R.J., et al. (2006), Investigating the causes of the response of the thermohaline circulation to  
 280 past and future climate changes, *J. Climate*, **19**, 1365-1387.

281 Swingedouw D., Braconnot P., Delecluse P., Guilyardi E., and Marti O., (2007), Quantifying the  
 282 AMOC feedbacks during a 2xCO<sub>2</sub> stabilization experiment with land-ice melting, *Climate*  
 283 *Dynamics*, **29**, 521-534.

284 Taylor, K.E., R.J. Stouffer, and G.A. Meehl (2012), An overview of CMIP5 and the experimental  
 285 design, *Bull. Amer. Met. Soc.*, **93**, 485-498.

286 de Vries, P., and S. L. Weber (2005), The Atlantic freshwater budget as a diagnostic for the existence  
 287 of a stable shut down of the meridional overturning circulation, *Geophys. Res. Lett.*, **32**,  
 288 L09606, doi:10.1029/2004GL021450

289 Weber, S. L., et al. (2007), The modern and glacial overturning circulation in the Atlantic Ocean in  
 290 PMIP coupled model simulations, *Climate of the Past*, **3**, 51-64.

291 Weijer, W., P.M. de Ruijter, H.A. Dijkstra, and P.J. van Leeuwen (1999), Impact of interbasin  
 292 exchange on the Atlantic overturning circulation, *J. Phys. Oceanogr.*, **29**, 2266-2284.

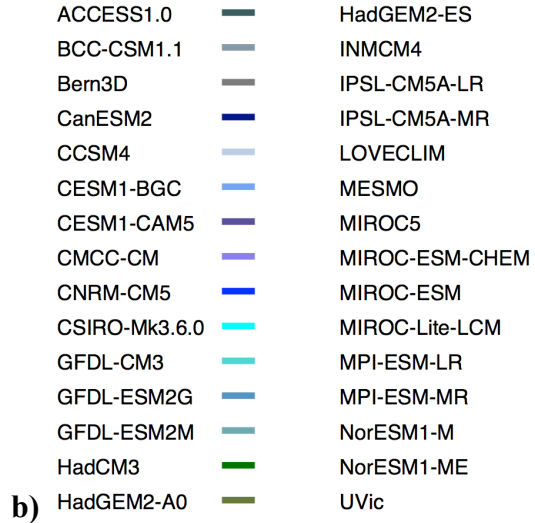
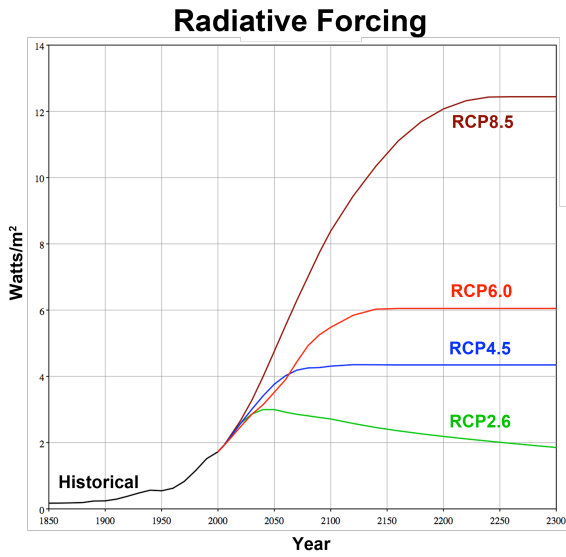
293 Zickfeld, K., et al. (2012), Long-term climate change commitment and reversibility, *J. Climate*,  
 294 submitted.

295

296 **Table 1:** Models for which the flux of freshwater into the Atlantic ( $F_{ov}$ ) at 30° or 32°S was calculated<sup>a</sup>.

Model Name	Country	Model type	RCP(s) used and the final year to which integration occurred in parentheses	Regime
ACCESS1.0	Australia	CMIP5	4.5 (2100); 8.5 (2100)	Bistable
BCC-CSM1.1	China	CMIP5	4.5 (2300); 6.0 (2100); 8.5 (2300)	Bistable
Bern3D	Switzerland	EMIC	2.6 (3000); 4.5 (3000); 6.0 (3000); 8.5 (3000)	Multiple
CanESM2	Canada	CMIP5	2.6 (2300); 4.5 (2300); 8.5 (2100)	Monostable
CCSM4	USA	CMIP5	4.5 (2300)	Monostable
CESM1-BGC	USA	CMIP5	4.5 (2100); 8.5 (2100)	Monostable
CESM1-CAM5	USA	CMIP5	4.5 (2300); 6.0 (2300); 8.5 (2100)	Monostable
CMCC-CM	Italy	CMIP5	4.5 (2100); 8.5 (2100)	Bistable
CNRM-CM5	France	CMIP5	2.6 (2100); 4.5 (2300); 8.5 (2300)	Monostable
CSIRO-MK3.6.0	Australia	CMIP5	2.6 (2100); 4.5 (2300); 6.0 (2100); 8.5 (2300)	Monostable
GFDL-CM3	USA	CMIP5	2.6 (2100); 4.5 (2100); 6.0 (2100); 8.5 (2100)	Bistable
GFDL-ESM2G	USA	CMIP5	2.6 (2100); 4.5 (2100); 6.0 (2100); 8.5 (2100)	Monostable
GFDL-ESM2M	USA	CMIP5	2.6 (2100); 4.5 (2100); 6.0 (2100); 8.5 (2100)	Multiple
HadCM3	UK	CMIP5	4.5 (2035)	Monostable
HadGEM2-AO	UK	CMIP5	2.6 (2100); 4.5 (2100); 6.0 (2100); 8.5 (2100)	Bistable
HadGEM2-ES	UK	CMIP5	2.6 (2300); 4.5 (2300); 6.0 (2100)	Monostable
INMCM4	Russia	CMIP5	4.5 (2100); 8.5 (2100)	Bistable
IPSL-CM5A-LR	France	CMIP5	2.6 (2300); 4.5 (2300); 6.0 (2100); 8.5 (2300)	Bistable
IPSL-CM5A-MR	France	CMIP5	2.6 (2100); 4.5 (2100); 8.5 (2100)	Bistable
LOVECLIM	Belgium	EMIC	2.6 (3000); 4.5 (3000); 6.0 (3000); 8.5 (3000)	Monostable
MESMO	USA	EMIC	2.6 (3000); 4.5 (3000); 6.0 (3000); 8.5 (3000)	Multiple
MIROC5	Japan	CMIP5	2.6 (2100); 4.5 (2100); 6.0 (2100); 8.5 (2100)	Bistable
MIROC-ESM-CHEM	Japan	CMIP5	2.6 (2100); 4.5 (2100); 6.0 (2100); 8.5 (2100)	Bistable
MIROC-ESM	Japan	CMIP5	2.6 (2100); 4.5 (2300); 6.0 (2100); 8.5 (2100)	Bistable
MIROC-Lite-LCM	Japan	EMIC	2.6 (3000); 4.5 (3000); 6.0 (3000); 8.5 (3000)	Monostable
MPI-ESM-LR	Germany	CMIP5	2.6 (2300); 4.5 (2300); 8.5 (2300)	Multiple
MPI-ESM-MR	Germany	CMIP5	2.6 (2100); 4.5 (2100); 8.5 (2100)	Bistable
NorESM1-M	Norway	CMIP5	2.6 (2100); 4.5 (2300); 6.0 (2100); 8.5 (2100)	Monostable
NorESM1-ME	Norway	CMIP5	4.5 (2100)	Monostable
UVic	Canada	EMIC	2.6 (3000); 4.5 (3000); 6.0 (3000); 8.5 (3000)	Bistable

<sup>a</sup>Not all models had maximum Atlantic MOC information available on the CMIP5 database. Columns 1-3 provide the model name, its country of origin and whether is is an EMIC or a CMIP5 model, respectively. The 4<sup>th</sup> column gives information on the RCPs used by each model and the final year of integration using that RCP (in parentheses). The 5<sup>th</sup> column indicates whether the model is always in a bistable or monostable regime for all RCPs. The entry *Multiple* indicates that at least for one RCP, the model moves from a bistable to a monostable regime or vice versa (see text for details).



305 a)

306 **Figure 1. a)** Net radiative forcing in Watts/m<sup>2</sup> over the historical period (1850-2005), 21<sup>st</sup> century  
 307 (2006–2100) and the RCP extension period (2100–2300). In the EMIC experiments that continued on  
 308 until 3000, the radiative forcing was held constant at 2300 values. **b)** Colour legend used in Figures 2  
 309 and 3. The five EMICs are: Bern3D, LOVECLIM, MESMO, MIROC-Lite-LCM, UVic.

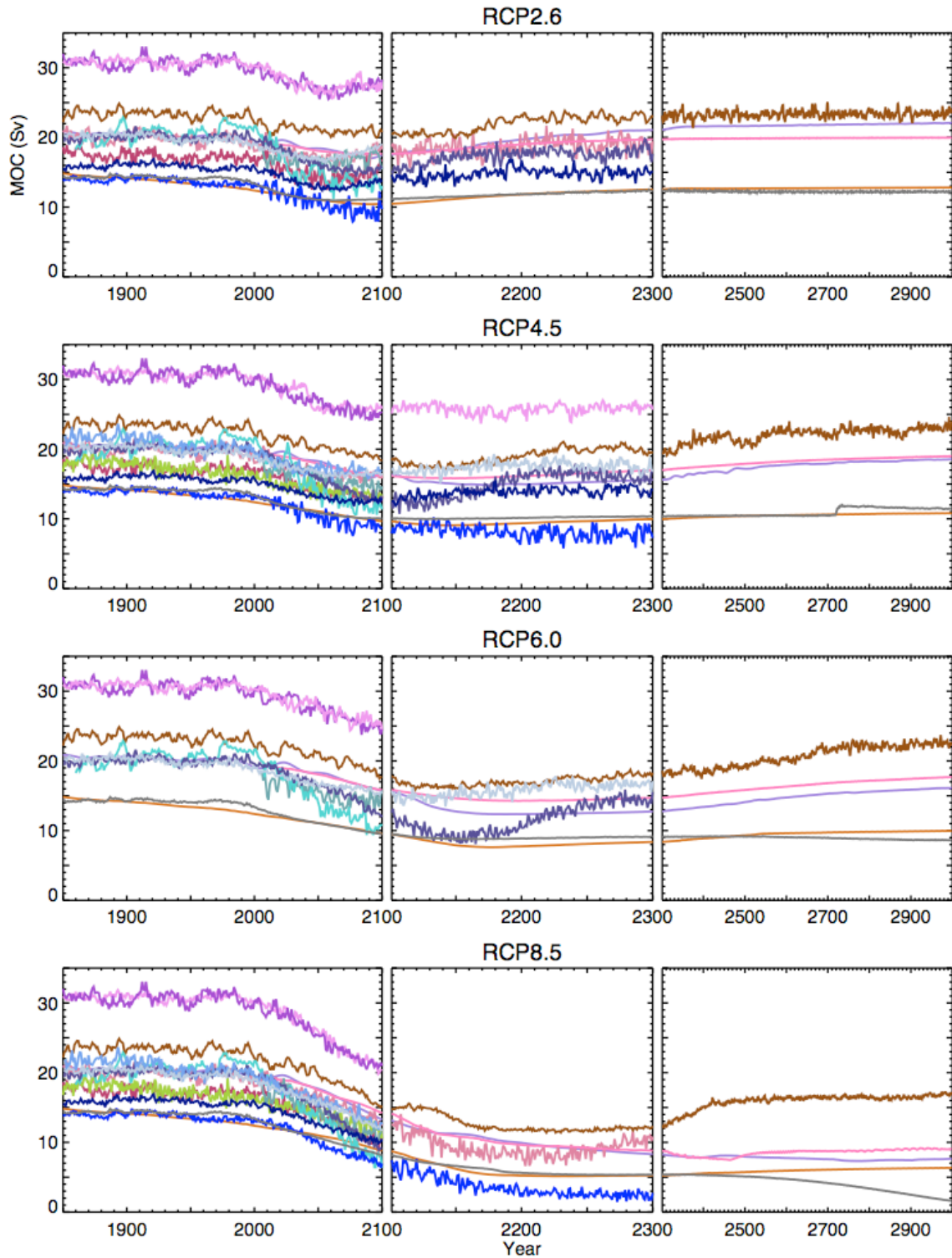


**Figure 2** Maximum strength of the Atlantic Meridional Overturning Circulation (AMOC) in Sv ( $1 \text{ Sv} \equiv 10^6 \text{ m}^3 \text{ s}^{-1}$ ) for the 5 EMICs and the 12 CMIP5 models (see Figure 1b for a colour legend). Each row shows the AMOC strength from 1850-2100 (column 1), 2100-2300 (column 2) and 2300-3000 (column 3) for a different Representative Concentration Pathway: RCP 2.6 (top); RCP 4.5 (second row); RCP 4.5 (third row); RCP 8.5 (bottom).

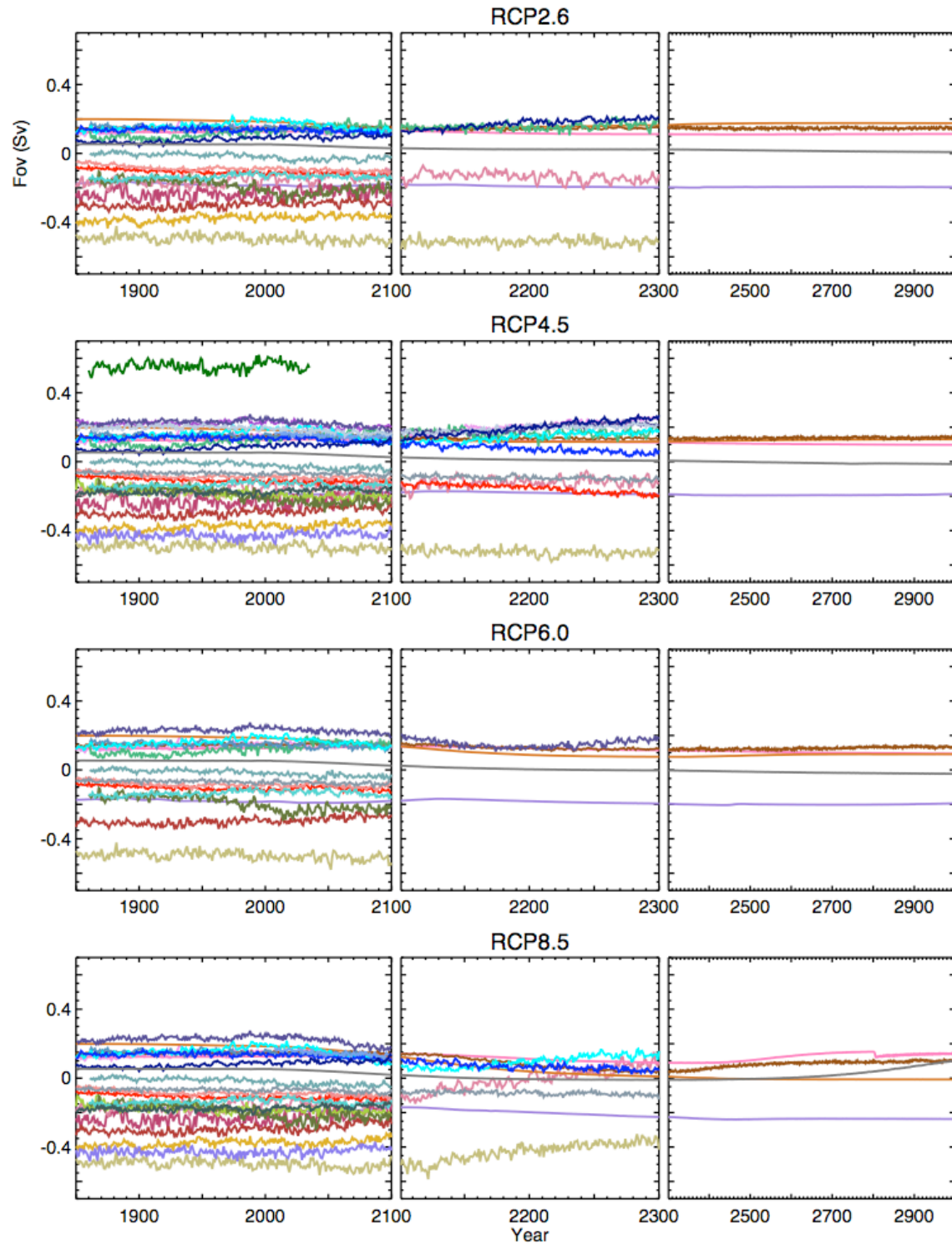


**Figure 3.** Flux of freshwater in Sv ( $1 \text{ Sv} \equiv 10^6 \text{ m}^3 \text{ s}^{-1}$ ) into the Atlantic ( $F_{\text{ov}}$ ) across  $30^\circ\text{S}$  for the 5 EMICs and across  $32^\circ\text{S}$  for the 25 CMIP5 models (see Figure 1b for a colour legend). Each row shows  $F_{\text{ov}}$  from 1850-2100 (column 1), 2100-2300 (column 2) and 2300-3000 (column 3) for a different Representative Concentration Pathway: RCP 2.6 (top); RCP 4.5 (second row); RCP 4.5 (third row); RCP 8.5 (bottom).

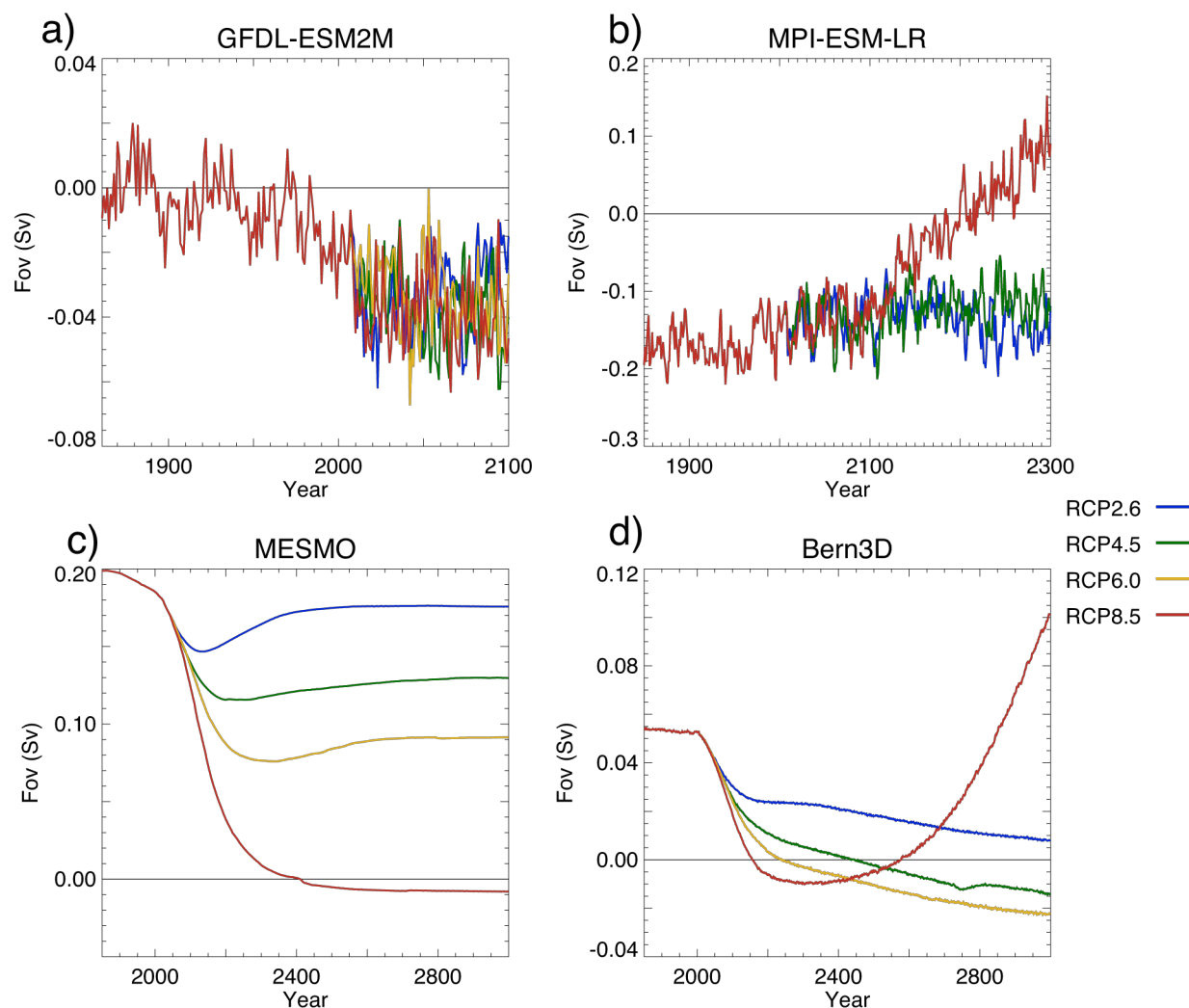


**Figure 4.** Flux of freshwater in Sv ( $1 \text{ Sv} \equiv 10^6 \text{ m}^3 \text{ s}^{-1}$ ) into the Atlantic ( $F_{ov}$ ) across 32°S for the **a)** GFDL-ESM2M and **b)** MPI-ESM-LR models, and across 30°S for the **c)** MESMO and **d)** Bern3D EMICs. The historical and all RCP integrations are shown on the same figure.